




Development of a permethylation-based detection method for oligo/polysialic acid structures via tandem MALDI-TOF mass spectrometry

Kai Suzuki^{a,1}, Di Wu^{a,b,1}, Ken Kitajima^b, Nao Yamakawa^{b,c}, Takayuki Omoto^b, Masaya Hane^{a,b}, Chihiro Sato^{a,b,*} 

^a Graduate School of Bioagricultural Sciences, Nagoya University, Nagoya, 464-8601, Japan

^b Integrated Glyco-Biomedical Research Center (iGMED), Institute for Glyco-core Research (iGCORE), Nagoya University, Nagoya, 464-8601, Japan

^c US 41-UAR 2014-PLBS, Université de Lille, CNRS, INSERM, CHU Lille, Institut Pasteur de Lille, Lille, France

ARTICLE INFO

Keywords:

Oligosialic acid
Polysialic acid
Permethylation
MALDI TOF/TOF
Mass spectrometry
Polysialoglycoprotein

ABSTRACT

Oligo/polysialic acid (oligo/polySia) refers to a class of linear polymers composed of Sias, found extensively at the non-reducing ends of glycans across various organisms, from bacteria to vertebrates. Different types of oligo/polySia have been characterized, varying in Sia composition, α -ketosidic linkages to penultimate Sia residues, and degree of polymerization. Detection of oligo/polySia-capped glycans is typically achieved through western blotting or ELISA using specific antibodies or endo-N-acetylneuraminidase. Additionally, a sensitive chemical approach involving the direct labeling of oligo/polySia with 1,2-diamino-4,5-methylenedioxybenzene, followed by separation and quantification via anion-exchange high-performance liquid chromatography, has been developed. However, detection through mass spectrometry (MS) has remained challenging due to the multiple negative charges and structural instability of these glycans. In this study, we applied a permethylation technique to convert carboxyl group of Sias into methyl esters, thereby neutralizing their negative charges, which allowed for improved MS analysis of sialylated glycans. We optimized both the permethylation and glycan purification processes. Consequently, we achieved the first successful detection of polySia structures using MALDI-TOF MS. There are more in-source decay ions in the MS profiling of permethylated α 2,9-linked polySias compared to α 2,8-linked polySias. Furthermore, we present the first examples of oligo/polySia sequencing by collision-induced dissociation on a TOF/TOF instrument, enabling us to differentiate between α 2,8- and α 2,9-linked polySias. We extended this approach to analyze oligo/polySia structures with O-linked glycans in polysialoglycoprotein from salmonid eggs. For the first time, the analysis of intact oligo/polySia structures with O-linked glycans were successfully detected using MALDI-TOF/TOF MS/MS with this optimized permethylation method.

Abbreviations

CID collision-induced dissociation
Kdn deaminoneuraminic acid
DBU 1,8-diazabicyclo[5.4.0] undec-7-ene
DMB 1,2-diamino-4,5-methylenedioxybenzene
DP degree of polymerization
HPLC high performance liquid chromatography
MS mass spectrometry
MS/MS tandem mass spectrometry
MALDI matrix assisted laser desorption/ionization

Neu5Ac N-acetylneuraminic acid
Neu5Gc N-glycolylneuraminic acid
oligoSia oligosialic acid
polySia polysialic acid
PSGP polysialoglycoprotein
TOF/TOF time-of-flight / time-of-flight

1. Introduction

Glycans are essential post-translational modifications of proteins, with 50 to 80 % of proteins modified by glycans, although their presence

* Corresponding author at: Integrated Glyco-Biomedical Research Center (iGMED), Institute for Glyco-core Research (iGCORE), Nagoya University, Nagoya, 464-8601, Japan.

E-mail address: chi@agr.nagoya-u.ac.jp (C. Sato).

¹ These authors are equally contributed to this work.

<https://doi.org/10.1016/j.bbadv.2025.100155>

Received 26 November 2024; Received in revised form 27 February 2025; Accepted 5 March 2025

Available online 7 March 2025

2667-1603/© 2025 The Authors. Published by Elsevier B.V. This is an open access article under the CC BY-NC-ND license (<http://creativecommons.org/licenses/by-nc-nd/4.0/>).

on proteins is often overlooked. Glycans fulfill numerous biological roles by influencing protein conformation and function, as well as through their specific function. Some glycans have been identified as biomarkers for diseases, including cancers. Recognized as the "third chain of life," glycans participate in critical biological processes. However, advancements in glycan analysis have lagged due to its complexity, especially when compared with the analysis of nucleotides (the "first chain of life") and proteins (the "second chain of life"). While genome and proteome analyses are now routine and yield valuable insights, glycan data remains relatively sparse. Recently, glycome analysis has made strides, with glycoproteome analyses using liquid chromatography-mass spectrometry (LC-MS)[1] and comprehensive glycomics[2] emerging as powerful tools for acquiring glycan information.

MALDI-based mass spectrometry (MS) has become a high-throughput, robust technique for glycomic analysis, frequently used as an initial screening tool to characterize glycan complexity. For MS-based glycomic analysis, detecting glycans can be challenging without labeling, such as with pyridylamine (PA)[3] or [N-((aminooxy)acetyl) tryptophylarginine methyl ester] (aoWR)[4]. Detection is particularly difficult for glycans with terminal sialic acids, even when labeled with PA or aoWR. The recently developed sialic acid linkage-specific alkylation (SALSA) method has improved the sensitive detection of sialic acids (Sias)[4]. Beyond SALSA, permethylation is widely employed in glycan structural analysis to neutralize the negative charges on sialylated glycans, facilitating MS analysis[5–7]. Methylation, a classical yet effective method, allows for straightforward MS detection of glycans. Recent MS-based glycomic advancements have enabled the detection of not only mono-sialylated glycans but also terminal disialic acid (diSia) substituents[8,9]. To detect longer polymeric forms of Sia, on-target lactonization has been employed via MS analysis[10,11], however, the lactonization via acidic conditions change the intact polySia structures.

PolySia consists of linear Sia polymers distributed across evolutionary lines, from bacteria to vertebrates[12,13]. PolySia displays significant structural diversity, primarily due to variations in α -ketosidic linkages to penultimate Sia residues (e.g., $\alpha 2 \rightarrow 8$, $\alpha 2 \rightarrow 9$, and $\alpha 2 \rightarrow 5$ -Oglycosyl) and in chain length or degree of polymerization (DP), which ranges from 8 to 400 residues[14–18]. Among these, the $\alpha 2 \rightarrow 8$ linkage is most common in animal glycoconjugates. PolySia with $\alpha 2 \rightarrow 8$ linkages was initially identified in polysialoglycoprotein (PSGP) from salmonid eggs[15,19] and later in neural cell adhesion molecule (NCAM) from the embryonic brains of rodents[20]. The $\alpha 2 \rightarrow 9$ -linked polySia was first identified in *Neisseria meningitidis* group C[21] and later in animal proteins, such as an unidentified protein in mouse neuroblastoma cells[15] and the sea urchin sperm flagella sialin[22,23].

PolySia has several unique biological functions attributed to its distinct properties[12,13]. One notable feature is its anti-adhesive effect. Due to its high hydration capacity, polySia disrupts NCAM-NCAM or NCAM-other molecule interactions, thereby modulating cell-cell interactions and influencing cell signaling strength. Another feature is its ability to bind specific molecules. PolySia can capture neurotrophic factors like brain-derived neurotrophic factor (BDNF), fibroblast growth factor (FGF), and dopamine (DA) depending on its degree of polymerization, serving as a reservoir for these critical neurological molecules [24,25]. Through these attributes, polySia is involved in numerous neural functions, such as memory, learning, circadian rhythm, and social behavior. Recently, structural abnormalities in polySia have been linked to various human diseases, including mental disorders and cancers[26]. Current methods for detecting polySia include Western blotting, ELISA, and anion exchange chromatography after labeling with DMB[15,27]; however, intact polySia has not yet been successfully analyzed using MS and MS/MS analysis. Thus, developing a highly sensitive MS-based approach for intact polySia structural detection is essential.

In this study, we report the first detection and differentiation of $\alpha 2,8$ - and $\alpha 2,9$ -linked polySia using MALDI-based MS following

permethylation. This MS-based method offers not only sensitive detection but also the ability to distinguish polySia linkage types and chain lengths. We applied this method to analyze polymerized Sia structures in PSGP derived from salmonid eggs, successfully detecting oligo/polySia structures with a DP of up to 7 on O-linked glycans of PSGP through MS-based analysis.

2. Results

2.1. Permethyated polySias were successfully detected using MALDI-TOF MS analysis

$\alpha 2,8$ -linked polySia ($\alpha 2,8$ -linked polyNeu5Ac) and $\alpha 2,9$ -linked polySia ($\alpha 2,9$ -linked polyNeu5Ac) (Fig. 1A), dissolved in Milli-Q water, were lyophilized in a glass tube and permethylated by first adding an anhydrous NaOH suspension in DMSO, followed by iodomethane. The permethylated $\alpha 2,8$ -linked and $\alpha 2,9$ -linked polySias (Fig. 1B) were analyzed using a MALDI-TOF MS instrument in positive ion linear mode (Fig. 2). Both $\alpha 2,8$ -linked polyNeu5Ac and $\alpha 2,9$ -linked polyNeu5Ac displayed typical MALDI spectra for methylated homopolymers, with a mass difference between adjacent peaks of 361, corresponding to the expected mass of permethylated monomeric Neu5Ac (monoNeu5Ac). The maximum DP observed for both $\alpha 2,8$ - and $\alpha 2,9$ -polySia was 41 (Fig. 2B). Notably, the DP of intact $\alpha 2,8$ -polyNeuAc was similar (DP=42) when analyzed by anion exchange chromatography[28]. This consistency indicates that polySia degradation did not occur during permethylation, and the method provides high detection sensitivity in MALDI-MS analysis.

The permethylated polySias (Fig. 1B) were further analyzed in positive ion reflector mode (Fig. 3). When 1 mM of sodium acetate was added to the matrix as a cation adduct, both the permethylated and oxonium forms of oligo/polySias (DP = 3 to 11) were detected, with a mass difference between them of 54. Interestingly, the ratios of oxonium ions to permethylated forms differed between $\alpha 2,8$ - and $\alpha 2,9$ -polySias (Fig. 3). For example, the ratios of oxonium ions to permethylated forms for $\alpha 2,8$ -linked (Neu5Ac)₃, (Neu5Ac)₄, and (Neu5Ac)₅ were 12/7, 1/2, and 2/7, respectively, whereas the corresponding ratios for $\alpha 2,9$ -linked (Neu5Ac)₃, (Neu5Ac)₄, and (Neu5Ac)₅ were 91/5, 41/3, and 23/5, respectively. A significantly higher amount of oxonium ions was observed in $\alpha 2,9$ -oligo/polySia, while only minimal oxonium ions were detected in $\alpha 2,8$ -oligo/polySia (DP = 3 to 11). Moreover, the MALDI-MS profiles for both $\alpha 2,8$ - and $\alpha 2,9$ -polySias remained consistent even as the amount of polySia used was reduced (Fig. S1).

2.2. MALDI TOF/TOF MS/MS fragmentation data analysis of the oxonium ion of $\alpha 2,8$ - and $\alpha 2,9$ -PolySia

In the second stage of the analysis, tandem MS (MS/MS) experiments were conducted on the oxonium ions of $\alpha 2,8$ - and $\alpha 2,9$ -oligo/polySia. The MS/MS profile for the ion at m/z 1098, corresponding to the oxonium ion of $\alpha 2,8$ -(Neu5Ac)₃, is shown in the upper panel of Fig. 4A, while the oxonium ion of $\alpha 2,9$ -(Neu5Ac)₃ is depicted in the lower panel. Oxonium type B₂ ion fragments at m/z 737 and Y₂ ion fragments at m/z 722 were observed (Fig. 4A and B), supporting a linear structure. Interestingly, the intensity ratio of B₂ to Y₂ ions differed between $\alpha 2,8$ - and $\alpha 2,9$ -(Neu5Ac)₃. In $\alpha 2,9$ -(Neu5Ac)₃, the B₂ and Y₂ ions derived from the oxonium ion appeared in nearly equal abundance, indicating a unique fragmentation pattern characteristic of $\alpha 2,9$ -(Neu5Ac)₃. This distinct fragmentation feature was also detected in the oxonium ions of other $\alpha 2,9$ -linked oligo/polySia (DP = 4 to 8) (Fig. S2A to Fig. S6A). Additionally, a characteristic fragment ion at m/z 416 (Fig. 4B) was identified exclusively in $\alpha 2,8$ -(Neu5Ac)₃, serving as a diagnostic marker for this structure. This characteristic fragment was similarly observed in other $\alpha 2,8$ -linked oligo/polySia but was absent in $\alpha 2,9$ -linked oligo/polySia (DP = 4 to 8) (Fig. S2A to Fig. S6A).

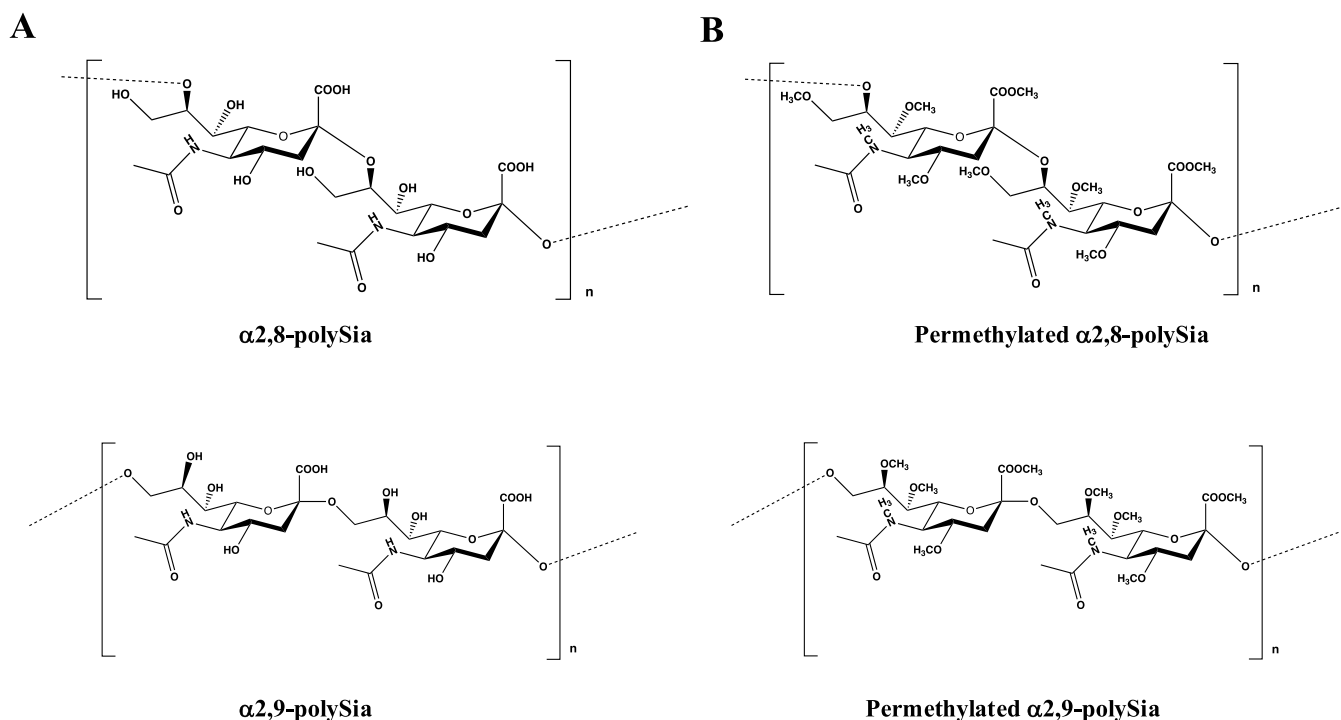


Fig. 1. Structure of polysialic acid. (A) Structures of α 2,8-linked polySia (upper) and α 2,9-linked polySia (lower). (B) Structures of permethylated α 2,8-linked polySia (upper) and α 2,9-linked polySia (lower).

2.3. MALDI TOF/TOF MS/MS fragmentation data analysis of permethylated α 2,8- and α 2,9-polySia

The MS/MS profile of the ion at m/z 1152, corresponding to the permethylated α 2,8-linked (Neu5Ac)₃, is shown in Fig. 5A (upper), with the profile for permethylated α 2,9-linked (Neu5Ac)₃ displayed in Fig. 5A (lower). In both permethylated α 2,8- and α 2,9-(Neu5Ac)₃ (Fig. 5), B₂ ion fragments at m/z 759 and Y₂ ion fragments at m/z 776 were detected, supporting a linear structure. B₁ ions appeared at m/z 376 and Y₁ ions appeared at m/z 416, along with their oxonium type at m/z 362. Additionally, the loss of a MeOH group from C4 occurs in some fragments, and were observed at m/z 344 and m/z 330, respectively (Fig. 5A). No significant differences were identified in the MS/MS fragmentation patterns between permethylated α 2,8- and α 2,9-(Neu5Ac)₃. MS/MS fragmentation data for other permethylated α 2,8- and α 2,9-polySias (DP = 4 to 8) are shown in Fig. S2B to Fig. S6B, where the B/Y ions characteristic of linear polySia were similarly detected.

2.4. Detection of oligo/polySia structures in O-linked glycans of PSGP

Following successful detection of free polySia chains by MALDI-TOF MS analysis, we extended this approach to detect naturally occurring polysialoglycoprotein (PSGP). PSGP was isolated from both unfertilized and fertilized eggs of lake trout (*Salvelinus namaycush*), a common constituent of Salmonidae fish eggs. PSGP is a highly glycosylated polypeptide with a molecular weight of 200 kDa (H-PSGP), low protein content (~15 % w/w), and high sialic acid (Neu5Ac) content (~30 % w/w)[15,29]. Each PSGP unit contains 3-O-glycosylation sites on serine or threonine residues, with each core oligosaccharide chain carrying an α 2,8-linked polymerized sialyl group, as illustrated in Fig. 6A[29]. In this first-time application of PSGP for MS analysis, we carefully optimized glycan purification steps, given that polymerized Sia structures are sensitive to acidic conditions and high temperatures (Fig. 6B). To analyze the oligosaccharide structures on PSGP, O-linked glycans were released from purified PSGP by β -elimination using hydroxylamine and the organic superbase 1,8-diazabicyclo[5.4.0]undec-7-ene (DBU)[30].

This method is comparable to β -elimination with anhydrous hydrazine but produces fewer degraded products. The released oligosaccharides were then purified using a HILIC column, with acidic, basic, and neutral conditions tested to optimize purification (Fig. 6B).

As shown in Fig. 7A and Fig. 8, five core oligosaccharide structures were identified: Hex₁(Neu5Ac)₂HexNAc₁ (Fig. 6A (a)) at m/z 1240 (H1N1S2), Hex₂(Neu5Ac)₂HexNAc₁ (Fig. 6A (b)) at m/z 1445 (H2N1S2), HexNAc₁Hex₂(Neu5Ac)_nHexNAc₁ (Fig. 6A (c)) at m/z 1329 (H2N2S1) and 1690 (H2N2S2), 2052 (H2N2S3), 2413 (H2N2S4), 2774 (H2N2S5), Fuc₁HexNAc₁Hex₂(Neu5Ac)_nHexNAc₁ (Fig. 6A (d)) at m/z 1142 (H2N2F1), 1864 (H2N2S2F1), 2226 (H2N2S3F1), 2587 (H2N2S4F1), 2948 (H2N2S5F1), and 3310 (H2N2S6F1) and HexNAc₁(Neu5Ac)₁HexNAc₁Hex₂(Neu5Ac)_nHexNAc₁ (Fig. 6A (e)) at m/z 1574 (H2N3S1), 1935 (H2N3S2), and 2297 (H2N3S3). These structures aligned with previously reported PSGP glycans[12,29] except for sialic acid species (Fig. 6A). The analyzed sample derived from Lake trout eggs whose sialic acid species was completely Neu5Ac[15]. Notably, the intensity of permethylated O-linked glycans was low when acidic purification (Method 1) was used (Fig. 7A), suggesting that acidic conditions, though common, were not ideal. Basic and neutral conditions provided better oligosaccharide isolation. Since the standard approach uses 5 % acetic acid for neutralization during the desalting step, which can degrade polymerized Sia structures, we reduced the volume of 5 % acetic acid to 0.5 ml for partial neutralization or omitted neutralization during desalting (Fig. 6B). As a result, polymerized Sia structures with a DP of up to 5 were clearly detected within the Fuc₁HexNAc₁Hex₂(Neu5Ac)_nHexNAc₁ core structures both with or without partial neutralization (Fig. 7C and Fig. S8). Finally, when 50 nmol of PSGP protein was analyzed by MALDI-TOF MS under optimized conditions (Method 2), we successfully detected oligo/polySia structures with a DP of up to 7 within the Fuc₁HexNAc₁Hex₂(Neu5Ac)_nHexNAc₁ core structures (Fig. 8).

3. Discussion

Permethylated is a widely used derivatization technique for

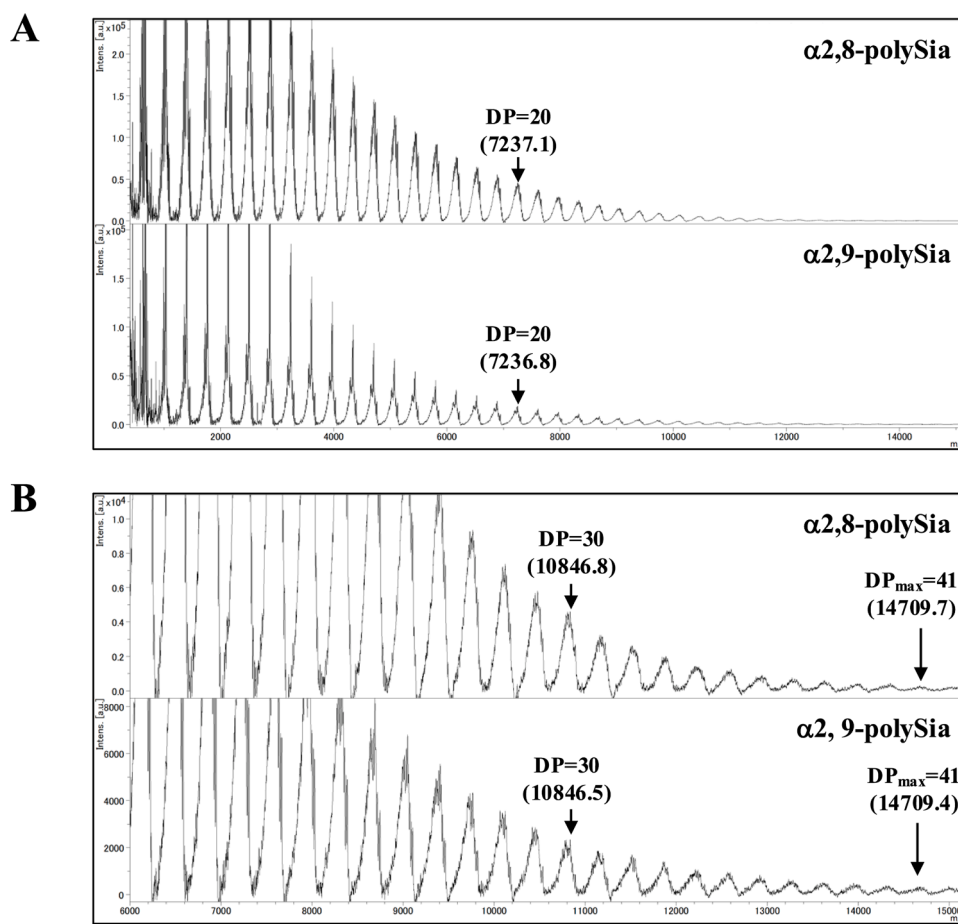


Fig. 2. MALDI-MS profile of permethylated polySia in linear positive ion mode. (A) MALDI-MS profile in the range of 1000–15,000 m/z. (B) MALDI-MS profile in the range of 6000–15,200 m/z. The upper panel shows α 2,8-linked polySia, and the lower panel shows α 2,9-linked polySia. Both α 2,8-linked polyNeu5Ac and α 2,9-linked polyNeu5Ac exhibit typical MALDI spectra for methylated homopolymers. The DP_{max} for both α 2,8- and α 2,9-linked polySia detected in linear positive ion mode was 41.

carbohydrate detection in MALDI-MS, as it enhances ionization efficiency and stabilizes sialic acid residues. Previously, this method was limited to detecting diSia on glycoconjugates, as polySia detection was challenging. In this study, we optimized permethylation conditions—including solution pH, incubation time, and temperature—which enabled the successful MS-based detection of oligo/polySias. The maximum DP for detected polySia was 41, consistent with results obtained via anion exchange chromatography[27,31]. The minimum amount of polySia required for MS analysis was 10 μ g, with typically 1/40 of the sample spotted on the target plate, resulting in a detection limit of 250 ng. This sensitivity exceeds that of TLC, which generally requires 1 μ g per spot and a minimum of 10 μ g of polySia for analysis. The sensitivity is also comparable to Fluorescent-Assisted detection by HPLC, which has a detection threshold of 100 ng[27,31].

During MALDI-MS detection, In-Source Decay (ISD) of permethylated polySia generated oxonium ions. Although excess sodium ions were incorporated into the matrix (DHB salt) to reduce protonation of permethylated glycans[32], only oxonium ions were detected for both in α 2,8-polySia and in α 2,9-polySia samples in linear positive ion mode, suggesting in-source decay happened when permethylated polySias were detected in linear mode (Fig. 2). On the other hand, a significantly greater number of oxonium ions were detected in α 2,9-polySia than in α 2,8-polySia samples in reflector positive ion mode (Fig. 3). The linkage type influenced the balance between cationization and protonation of polySia. Moreover, MS/MS fragmentation of oxonium ions from α 2,9-polySia produced diagnostic fragments that allowed differentiation between α 2,8- and α 2,9-linked polySias. This is the first instance of

distinguishing α 2,8 and α 2,9 sialic acid linkages using MS-based analysis. Specifically, MALDI TOF/TOF MS/MS fragmentation of the oxonium ion enables differentiation, with α 2,8-polySia producing a characteristic fragment ion at m/z 416, while α 2,9-polySia yields both B and Y ions with similar intensity. Given that polySia exhibits variations in α -ketosidic linkages to penultimate Sia residues, it would be interesting to test whether this optimal permethylation method can distinguish polySia connected by alternative linkages, such as α 2 \rightarrow 4, and α 2 \rightarrow 5-O_{glycoyl} or mixed α 2,8/9-linkages.

This study also marks the first characterization of O-linked glycans from purified lake trout PSGP protein using MS-based analysis. We used hydroxylamine and the organic superbase DBU to release O-linked glycans via β -elimination, which reduces degradation compared to traditional hydrazinolysis[30]. For oligo/polySia detection on O-linked glycans in PSGP, permethylation was optimized, allowing us to detect oligo/polySia structures with a DP up to 7, extending within the core glycan structure Fuc₁HexNAC₁Hex₂(Neu5Ac)_nHexNAC₁(Fig. 8B). In the previous report, the polySia structures in PSGP proteins isolated from unfertilized and fertilized eggs of brook trout (*Salvelinus fontinalis*) and rainbow trout (*Oncorhynchus mykiss*) were identified as homo- and heteropolymers of Neu5Gc and capping with or without Kdn[29]. In contrast, this study determined via MS analysis that the polySia structures in PSGP proteins isolated from lake trout eggs are homopolymers of Neu5Ac without Kdn capping. This is the same results obtained from previous work[15]. These findings again confirm that not linkage but the polySia species on PSGP vary depending on the fish species. This method demonstrated superior sensitivity compared to TLC and

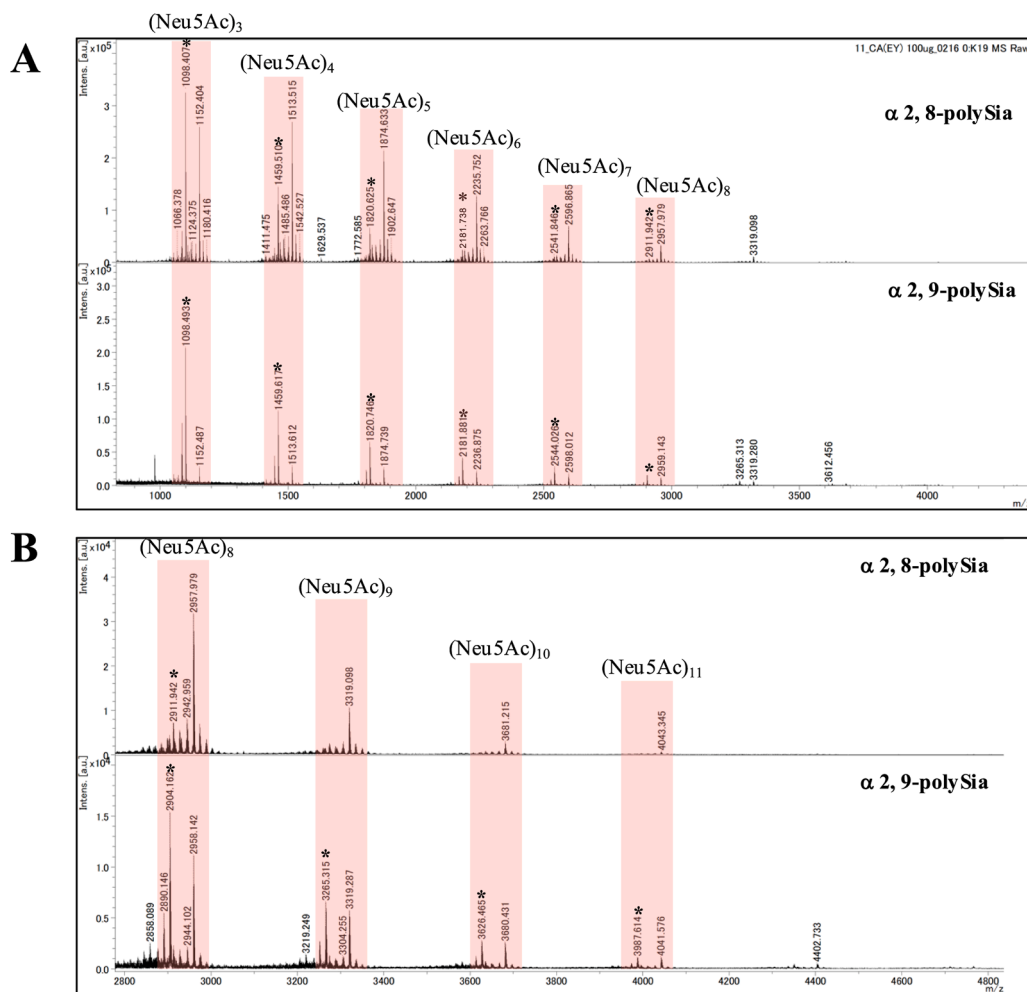


Fig. 3. MALDI-MS profile of permethylated polySia in reflector positive ion mode. (A) MALDI-MS profile in the range of 800–4800 m/z. (B) MALDI-MS profile in the range of 2800–4800 m/z. Permethylation was performed on 100 μg of polySia, with 1/40 of the sample spotted on the target plate. The upper panel shows α2,9-polySia, and the lower panel shows α2,8-polySia. Each $[M+Na]^+$ oligo/polySia molecular ion signal was labeled and confirmed by subsequent MS/MS analysis. Oxonium ions for each oligo/polySia are marked with an asterisk (*).

comparative to Fluorescent-Assisted detection by HPLC, offering an effective approach for detailed structural analysis of oligo/polySia on glycoconjugates.

4. Materials and methods

4.1. Materials

Acetone, acetonitrile, super dehydrated DMSO, acetic acid, iodomethane (CH₃I), chloroform, 50 % hydroxylamine, 2-propanol, and ammonia solution were obtained from Fujifilm Wako Pure Chemical Co. (Osaka, Japan). Sodium hydroxide (NaOH) powder was purchased from Sigma-Aldrich (St. Louis, MO, USA). α2,8-linked polySia (colominic acid from *E. coli*) was acquired from EY Laboratories (CA, USA), and α2,9-polySia from *Neisseria meningitidis* Group C was purified as previously reported[33]. 1,8-diazabicyclo[5.4.0]undec-7-ene (DBU) was sourced from Tokyo Chemical Industry Co., Ltd. (Tokyo, Japan). 2,5-Dihydroxybenzoic Acid (DHB) was purchased from Shimadzu (Kyoto, Japan), and the MonoSpin HILIC column from GL Sciences (Tokyo, Japan). The PSGP protein was isolated from unfertilized and fertilized eggs of lake trout (*S. namaycush*) as previously reported[15].

4.2. O-linked glycan liberation

To liberate O-linked glycans, 10 μL of a 50 % hydroxylamine solution

and 20 μL of DBU were added to a 20 μL glycoprotein solution containing 1–50 nmol of purified PSGP protein. The mixture was heated at 50 °C for 20 min, then transferred into 250 μL of cold acetone, followed by dilution with 6 mL of acetonitrile. The solution was applied to a MonoSpin HILIC column, pre-equilibrated with buffers A and B, followed by two washes with buffer C. The O-linked glycans were then eluted with buffer B and subsequently lyophilized. The buffers used for the acidic, basic, and neutral conditions are detailed in the following table:

	Acidic condition	Basic condition	Neutral condition
Buffer A	Acetonitrile:Milli-Q:2.5 % acetic acid = 95:4:1	Acetonitrile:Milli-Q = 95:5	Acetonitrile:Milli-Q = 95:5
Buffer B	Acetonitrile:Milli-Q:2.5 % acetic acid = 4:95:1	Acetonitrile:Milli-Q:2.5 % Ammonia = 4:95:1	Acetonitrile:Milli-Q = 5:95
Buffer C	Acetonitrile:2-Propanol:2.5 % acetic acid = 49.5:49.5:1	Acetonitrile:2-Propanol:Milli-Q = 49.5:49.5:1	Acetonitrile:2-Propanol:Milli-Q = 49.5:49.5:1

To optimize the detection of oligo/polySia structures in the released O-linked glycans from PSGP, six different methods were evaluated:

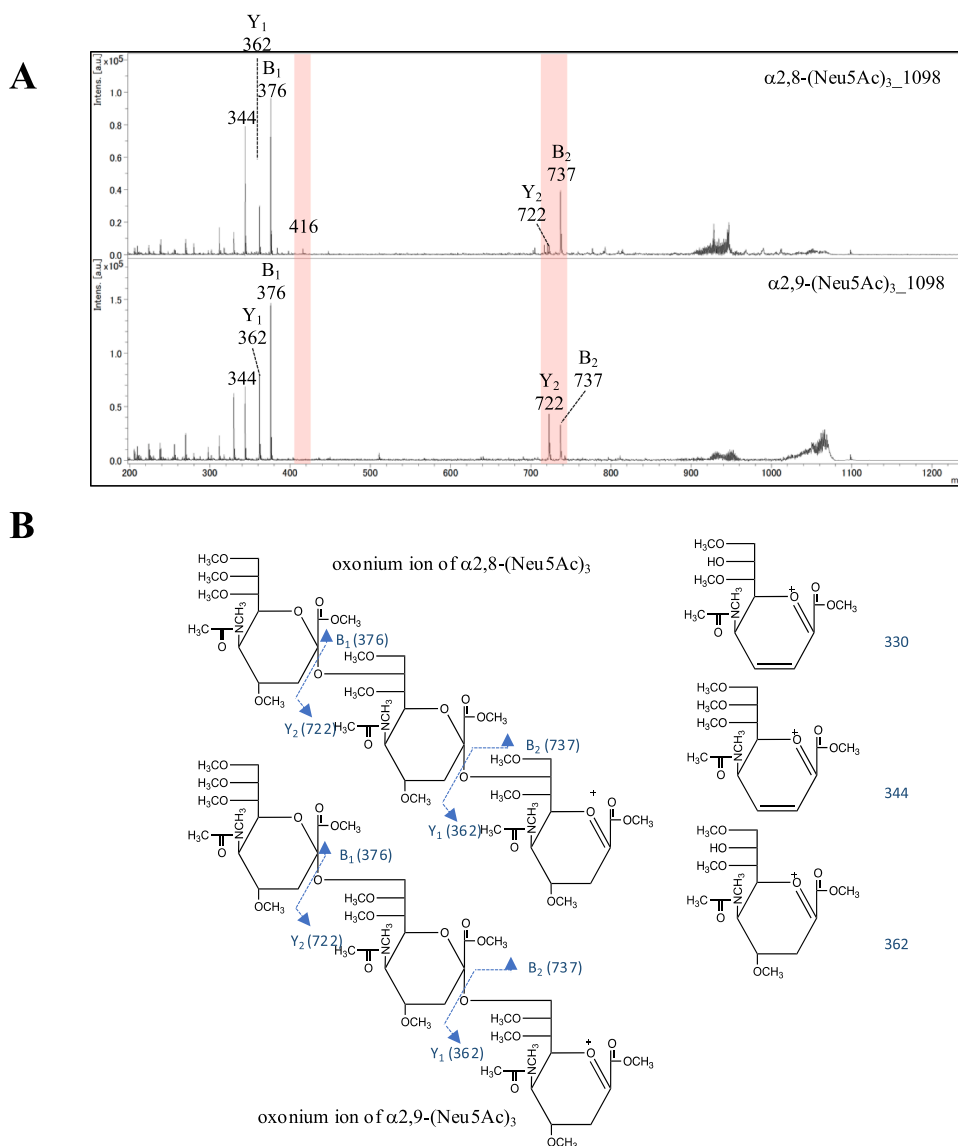


Fig. 4. MALDI TOF/TOF MS/MS profile of the oxonium ion of (Neu5Ac)₃. (A) The parent ions selected for MS/MS correspond to the oxonium ion of (Neu5Ac)₃ at m/z 1098. The upper panel shows $\alpha 2,8$ -linked (Neu5Ac)₃, and the lower panel shows $\alpha 2,9$ -linked (Neu5Ac)₃. (B) Characteristic fragment ions obtained by MALDI-TOF/TOF MS/MS analysis of the oxonium ion of (Neu5Ac)₃. Major signal assignments are schematically illustrated on the structures, with key ions labeled and the diagnostic markers were labeled by pink color.

- **Method 1:** O-linked glycans were purified on a HILIC column under acidic conditions. After permethylation, desalting was performed without neutralizing the excess NaOH.
- **Method 2:** O-linked glycans were purified on a HILIC column under basic conditions. After permethylation, desalting was performed without neutralizing the excess NaOH.
- **Method 3:** O-linked glycans were purified on a HILIC column under neutral conditions. After permethylation, desalting was performed without neutralizing the excess NaOH.
- **Method 4:** O-linked glycans were purified on a HILIC column under acidic conditions. After permethylation, excess NaOH was neutralized with 0.5 mL of 5 % acetic acid for desalting.
- **Method 5:** O-linked glycans were purified on a HILIC column under basic conditions. After permethylation, excess NaOH was neutralized with 0.5 mL of 5 % acetic acid for desalting.
- **Method 6:** O-linked glycans were purified on a HILIC column under neutral conditions. After permethylation, excess NaOH was neutralized with 0.5 mL of 5 % acetic acid for desalting.

4.3. Permethylation

PolySias (10–100 μg) were permethylated using the NaOH/DMSO method. $\alpha 2,8$ polySia and $\alpha 2,9$ polySia were dissolved in 0.4 ml of anhydrous DMSO. To this solution, 20 mg of finely powdered NaOH was added, and the mixture was vortexed thoroughly to create a NaOH/DMSO slurry. Immediately, 0.2 ml of iodomethane was added, and the air inside the glass tube was replaced with nitrogen gas. The reaction mixture was stirred at 200 rpm at 25 °C for 2 h. Excess NaOH was neutralized by adding 0.5 ml of 5 % acetic acid. The permethylated derivatives were then extracted with chloroform and washed repeatedly with water. The chloroform layer containing the permethylated glycans was transferred to a new sample tube, and the chloroform was evaporated to dryness.

4.4. MS and MS/MS analysis

Permethylated glycans were dissolved in 20 μl of acetonitrile, and 1 μl of this sample was mixed 1:1 with DHB solution (10 mg/ml in 50 %

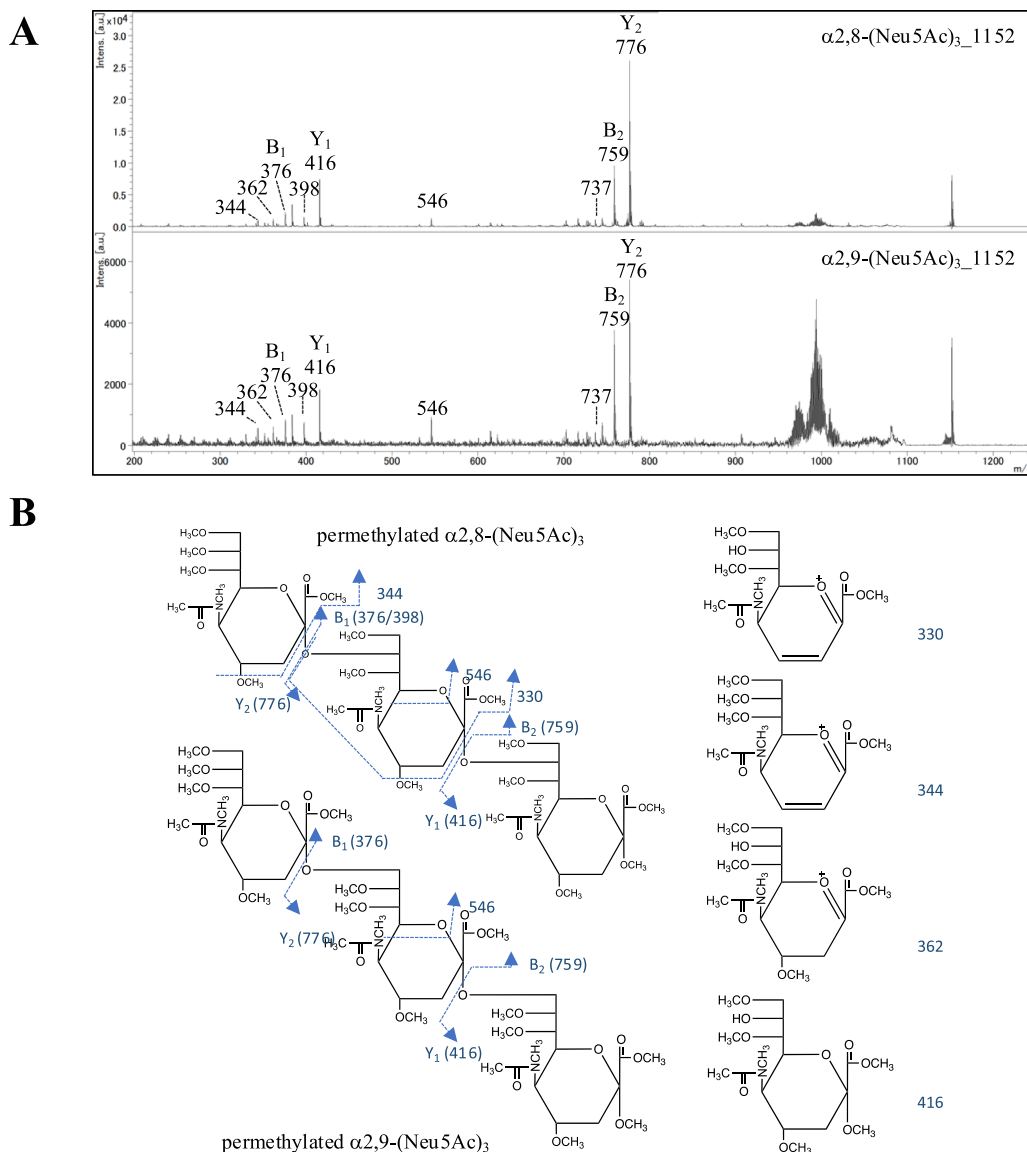


Fig. 5. MALDI TOF/TOF MS/MS profile of permethylated (Neu5Ac)₃. (A) The parent ions selected for MS/MS correspond to the permethylated ion of (Neu5Ac)₃ at *m/z* 1152. The upper panel shows α 2,8-linked (Neu5Ac)₃, and the lower panel shows α 2,9-linked (Neu5Ac)₃. (B) Characteristic fragment ions obtained by MALDI-TOF/TOF MS/MS analysis of permethylated (Neu5Ac)₃. Major signal assignments are schematically illustrated on the structures, with key ions labeled.

acetonitrile with 1 mM sodium acetate) before spotting onto the target plate. MALDI-MS and MALDI-MS/MS analyses were conducted on an UltrafleXtreme TOF/TOF-MS instrument equipped with a reflector, controlled by FlexControl 3.0 software (Bruker Daltonics, Bremen, Germany). All spectra were acquired in linear positive ion mode with an acceleration voltage of 20 kV, a reflector voltage of 0 kV, and a pulsed-ion extraction of 250 ns in positive-ion mode. All spectra were acquired in reflector mode with an acceleration voltage of 20 kV, a reflector voltage of 20.8 kV, and a pulsed-ion extraction of 320 ns in positive-ion mode. MS survey and CID MS/MS data were collected manually using FlexAnalysis 3.0 software. Argon served as the collision gas, with collision energy manually adjusted (between 100 and 400 V) to achieve the optimal degree of fragmentation.

CRediT authorship contribution statement

Kai Suzuki: Writing – review & editing, Writing – original draft, Validation, Methodology, Funding acquisition. **Di Wu:** Writing – review & editing, Writing – original draft, Validation, Methodology, Investigation, Funding acquisition, Formal analysis, Data curation. **Ken**

Kitajima: Writing – review & editing, Writing – original draft, Methodology, Data curation. **Nao Yamakawa:** Writing – review & editing, Writing – original draft, Validation, Data curation. **Takayuki Omoto:** Writing – original draft, Validation, Data curation. **Masaya Hane:** Writing – review & editing, Writing – original draft, Validation, Data curation. **Chihiro Sato:** Writing – review & editing, Writing – original draft, Validation, Supervision, Methodology, Investigation, Funding acquisition, Formal analysis, Data curation, Conceptualization.

Declaration of competing interest

The authors declare the following financial interests/personal relationships which may be considered as potential competing interests:

Chihiro SATO reports financial support was provided by Japan Agency for Medical Research and Development Department of Industrial Academic Collaboration. Chihiro SATO reports financial support was provided by Government of Japan Ministry of Education Culture Sports Science and Technology. Kai Suzuki reports financial support was provided by Government of Japan Ministry of Education Culture Sports Science and Technology. Masaya Hane reports financial support was

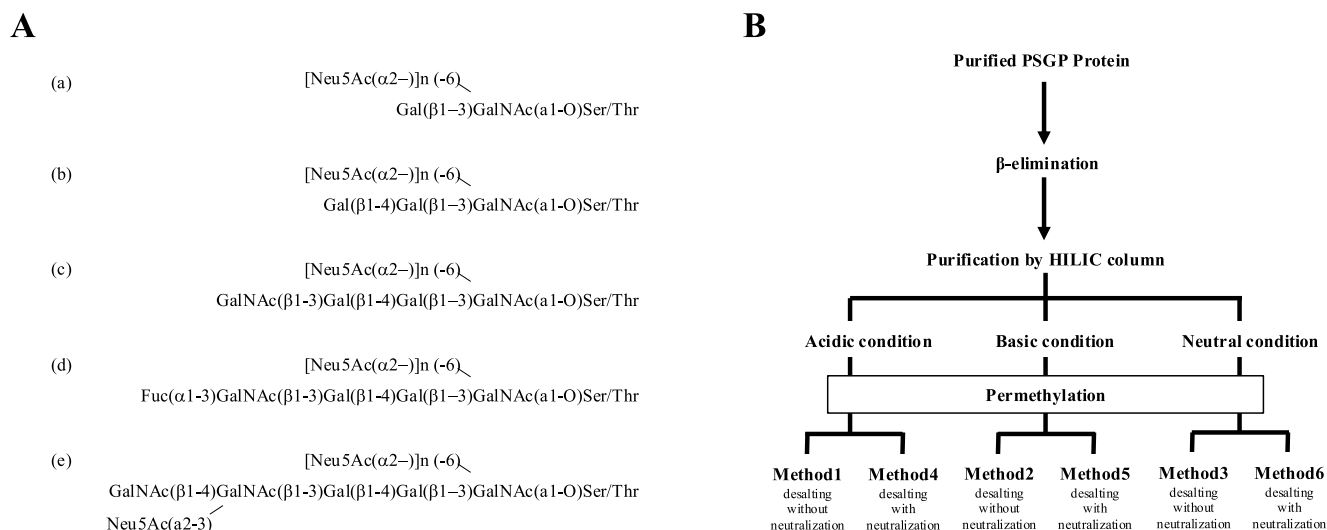


Fig. 6. Analytical scheme of O-linked glycans in PSGP derived from salmonid fish eggs. (A) Chemical structures of O-linked glycans in polysialoglycoprotein (PSGP) derived from salmonid fish eggs[15]. (B) Flowchart for detecting oligo/polySia structures in O-linked glycans released from PSGP. Different conditions for glycan purification via HILIC column and desalting for permethylation were tested as described in Methods.

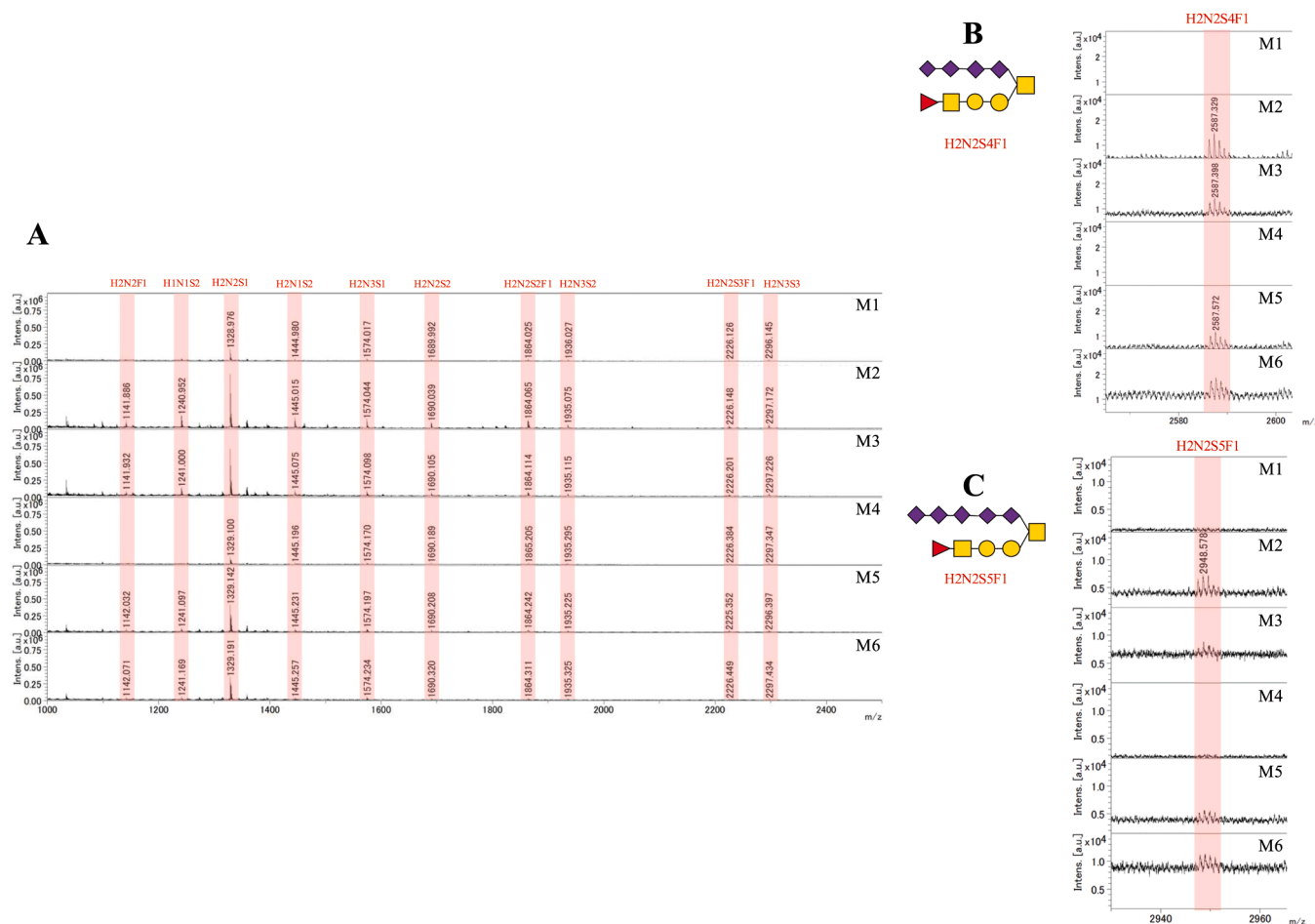


Fig. 7. (A) Comparison of MALDI-MS profiles of permethylated O-linked glycans in PSGP obtained by Method 1 (M1), Method 2 (M2), and Method 3 (M3), Method 4 (M4), Method 5 (M5) and Method 6 (M6). MALDI-MS profile of (A) in the range of 2565–2600 m/z was showed in B, and MALDI-MS profile of (A) in the range of 2930–2965 m/z was showed in C. The molecular compositions of major $[M+Na]^+$ molecular ion signals were assigned and confirmed by MS/MS analyses using MALDI-TOF/TOF, facilitating determination of the sequence and branching patterns of each detected O-linked glycan. Symbols used in this and other MS figures: square for HexNAc, circle for Hex, diamond for Neu5Ac. Peak annotations: F for Fucose, S for Neu5Ac, H for Hex, and N for HexNAc.

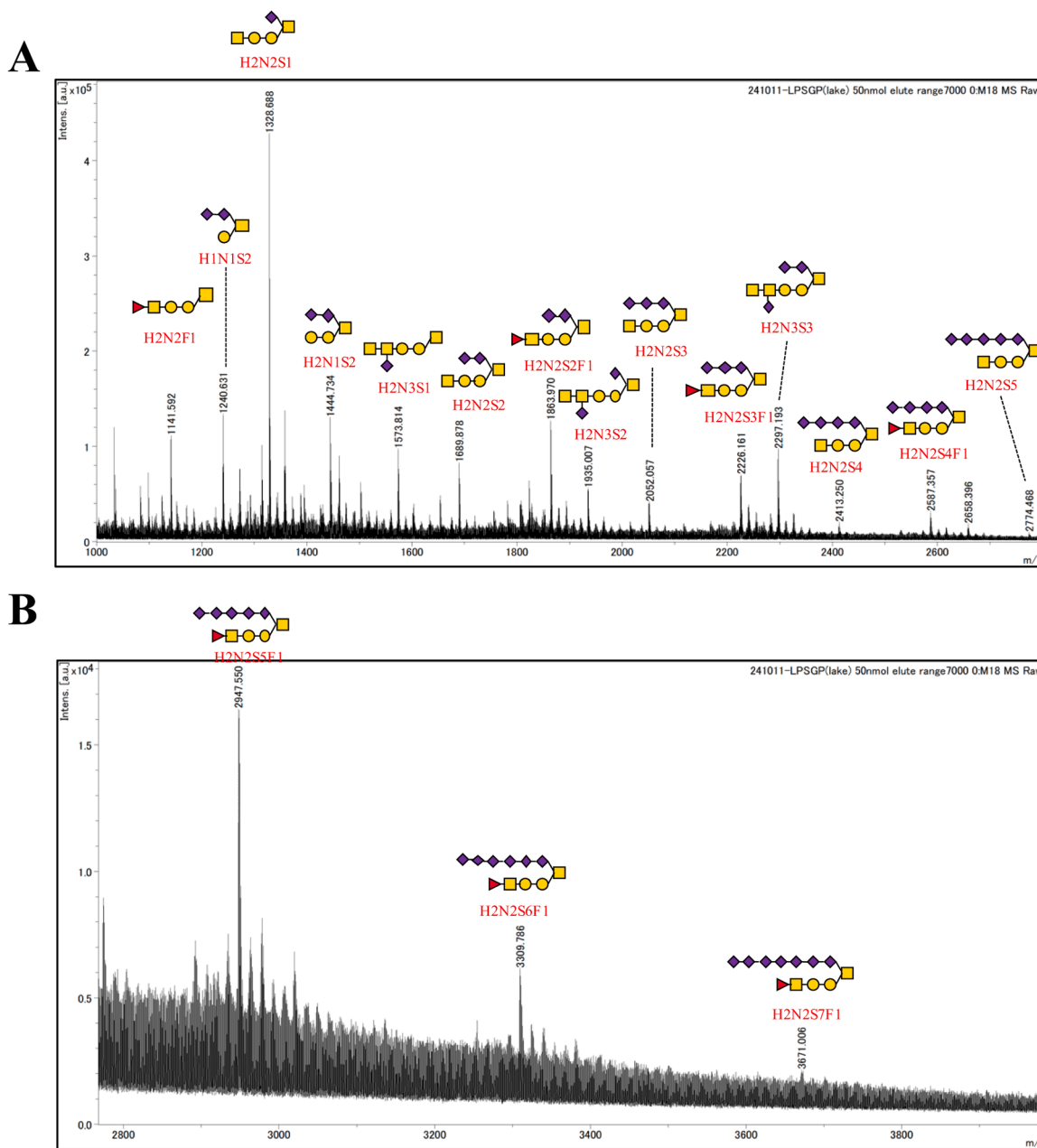


Fig. 8. MALDI-MS profile of permethylated *O*-linked glycans released from 50 nmol of PSGP. (A) MALDI-MS profile in the range of 1000–3700 *m/z*. (B) MALDI-MS profile in the range of 2600–4000 *m/z*. Major $[M+Na]^+$ molecular ion signals were assigned as labeled and confirmed by MS/MS analyses using MALDI-TOF/TOF, enabling detailed determination of the sequence and branching patterns of each detected *O*-linked glycan. Symbols used here and in other MS figures demonstrated in Fig. 7.

provided by Government of Japan Ministry of Education Culture Sports Science and Technology. Di Wu reports financial support was provided by Novartis Pharma SAS. If there are other authors, they declare that they have no known competing financial interests or personal relationships that could have appeared to influence the work reported in this paper.

Acknowledgements

This research was funded by Japan Agency for Medical Research and Development (AMED) grant number [18ae0101069h0003; 19ae0101069h0004; 20ae0101069h0005; 20gm6410007h0001; 21gm6410007h0002; 22gm6410007h0003; and 23gm6410007h0004] (to CS) and a Grant-in-Aid for Scientific Research(B)(21H02425 and

23K21291) from JSPS (to CS). A part of this research was also funded by CIBOG program (to KS). This work was also supported by Novartis Research Grants from The Novartis Foundation (to DW) and grant-in-Aid for Early-Career Scientists (22K15059), grant-in-Aid for Scientific Research C (24K08829) and the 34th The Naito Research Grant to MH. A part of this work is supported by J-Glyconet (JGN) and human glycome atlas project (HGA).

Supplementary materials

Supplementary material associated with this article can be found, in the online version, at [doi:10.1016/j.bbadv.2025.100155](https://doi.org/10.1016/j.bbadv.2025.100155).

Data availability

Data will be made available on request.

References

- [1] A. Chernykh, R. Kawahara, M. Thaysen-Andersen, Towards structure-focused glycoproteomics, *Biochem. Soc. Trans.* 49 (1) (2021) 161–186.
- [2] J.I. Furukawa, K. Okada, Y. Shinohara, Glycomics of human embryonic stem cells and human induced pluripotent stem cells, *Glycoconj. J.* 34 (6) (2017) 807–815.
- [3] H. Korekane, A. Matsumoto, F. Ota, et al., Involvement of ST6Gal I in the biosynthesis of a unique human colon cancer biomarker candidate, alpha2,6-sialylated blood group type 2H (ST2H) antigen, *J. Biochem.* 148 (3) (2010) 359–370.
- [4] H. Hanamatsu, T. Nishikaze, H. Tsumoto, et al., Comparative glycomic analysis of sialyl linkage isomers by sialic acid linkage-specific alkylamidation in combination with stable isotope labeling of α 2,3-linked sialic acid residues, *Anal. Chem.* 91 (21) (2019) 13343–13348.
- [5] Yu SY, S.W. Wu, K.H. Khoo, Distinctive characteristics of MALDI-Q/TOF and TOF/TOF tandem mass spectrometry for sequencing of permethylated complex type N-glycans, *Glycoconj. J.* 23 (5–6) (2006) 355–369.
- [6] K.H. Khoo, S.Y. Yu, Mass spectrometric analysis of sulfated N- and O-glycans, *Methods Enzymol.* 478 (2010) 3–26.
- [7] K.H. Khoo, A mass spectrometry-based glycopeptide-centric cellular glycomics is the more fruitful way forward to see the forest for the trees, *Biochem. Soc. Trans.* 49 (1) (2021) 55–69.
- [8] K. Canis, T.A. McKinnon, A. Nowak, et al., The plasma von Willebrand factor O-glycome comprises a surprising variety of structures including ABH antigens and disialosyl motifs, *J. Thromb. Haemost.* 8 (1) (2010) 137–145.
- [9] S.H. Wang, C.M. Tsai, K.I. Lin, K.H. Khoo, Advanced mass spectrometry and chemical analyses reveal the presence of terminal disialyl motif on mouse B-cell glycoproteins, *Glycobiology* 23 (6) (2013) 677–689.
- [10] S.P. Galuska, H. Geyer, C. Bleckmann, et al., Mass spectrometric fragmentation analysis of oligosialic and polysialic acids, *Anal. Chem.* 82 (5) (2010) 2059–2066.
- [11] S.P. Galuska, R. Geyer, M. Mühlhoff, H. Geyer, Characterization of oligo- and polysialic acids by MALDI-TOF-MS, *Anal. Chem.* 79 (18) (2007) 7161–7169.
- [12] C. Sato, K. Kitajima, Disialic, oligosialic and polysialic acids: distribution, functions and related disease, *J. Biochem.* 154 (2) (2013) 115–136.
- [13] C. Sato, K. Kitajima, Sialic acids in neurology, *Adv. Carbohydr. Chem. Biochem.* 76 (2019) 1–64.
- [14] M.N. Fukuda, A. Dell, J.E. Oates, M. Fukuda, Embryonal lactosaminoglycan. The structure of branched lactosaminoglycans with novel disialosyl (sialyl alpha 2—9 sialyl) terminals isolated from PA1 human embryonal carcinoma cells, *J. Biol. Chem.* 260 (11) (1985) 6623–6631.
- [15] C. Sato, K. Kitajima, I. Tazawa, Y. Inoue, S. Inoue, F.A. Troy, Structural diversity in the alpha 2—8-linked polysialic acid chains in salmonid fish egg glycoproteins. Occurrence of poly(Neu5Ac), poly(Neu5Gc), poly(Neu5Ac, Neu5Gc), poly(KDN), and their partially acetylated forms, *J. Biol. Chem.* 268 (31) (1993) 23675–23684.
- [16] S. Kitazume, K. Kitajima, S. Inoue, et al., Identification of polysialic acid-containing glycoprotein in the jelly coat of sea urchin eggs. Occurrence of a novel type of polysialic acid structure, *J. Biol. Chem.* 269 (36) (1994) 22712–22718.
- [17] T. Ijuin, K. Kitajima, Y. Song, et al., Isolation and identification of novel sulfated and nonsulfated oligosialyl glycosphingolipids from sea urchin sperm, *Glycoconj. J.* 13 (3) (1996) 401–413.
- [18] C. Sato, S. Inoue, T. Matsuda, K. Kitajima, Fluorescent-assisted detection of oligosialyl units in glycoconjugates, *Anal. Biochem.* 266 (1) (1999) 102–109.
- [19] S. Inoue, M. Iwasaki, Isolation of a novel glycoprotein from the eggs of rainbow trout: occurrence of disialosyl groups on all carbohydrate chains, *Biochem. Biophys. Res. Commun.* 83 (3) (1978) 1018–1023.
- [20] J. Finne, Occurrence of unique polysialosyl carbohydrate units in glycoproteins of developing brain, *J. Biol. Chem.* 257 (20) (1982) 11966–11970.
- [21] A.K. Bhattacharjee, H.J. Jennings, C.P. Kenny, A. Martin, I.C. Smith, Structural determination of the sialic acid polysaccharide antigens of *Neisseria meningitidis* serogroups B and C with carbon 13 nuclear magnetic resonance, *J. Biol. Chem.* 250 (5) (1975) 1926–1932.
- [22] S. Miyata, C. Sato, S. Kitamura, M. Toriyama, K. Kitajima, A major flagellum sialoglycoprotein in sea urchin sperm contains a novel polysialic acid, an alpha2,9-linked poly-N-acetylneuraminic acid chain, capped by an 8-O-sulfated sialic acid residue, *Glycobiology* 14 (9) (2004) 827–840.
- [23] S. Miyata, C. Sato, H. Kumita, M. Toriyama, V.D. Vacquier, K. Kitajima, Flagellin: a novel sulfated alpha2,9-linked polysialic acid glycoprotein of sea urchin sperm flagella, *Glycobiology* 16 (12) (2006) 1229–1241.
- [24] S. Ono, M. Hane, K. Kitajima, C. Sato, Novel regulation of fibroblast growth factor 2 (FGF2)-mediated cell growth by polysialic acid, *J. Biol. Chem.* 287 (6) (2012) 3710–3722.
- [25] M. Hane, S. Matsuoka, S. Ono, S. Miyata, K. Kitajima, C. Sato, Protective effects of polysialic acid on proteolytic cleavage of FGF2 and proBDNF/BDNF, *Glycobiology* 25 (10) (2015) 1112–1124.
- [26] C. Sato, K. Kitajima, Polysialylation and disease, *Mol. Aspects. Med.* 79 (2021) 100892.
- [27] A. Mori, Y. Yang, Y. Takahashi, M. Hane, K. Kitajima, C. Sato, Combinational analyses with multiple methods reveal the existence of several forms of polysialylated neural cell adhesion molecule in mouse developing brains, *Int. J. Mol. Sci.* 21 (16) (2020).
- [28] Y. Kanato, K. Kitajima, C. Sato, Direct binding of polysialic acid to a brain-derived neurotrophic factor depends on the degree of polymerization, *Glycobiology* 18 (12) (2008) 1044–1053.
- [29] K. Kitajima, Y. Inoue, S. Inoue, Polysialoglycoproteins of Salmonidae fish eggs. Complete structure of 200-kDa polysialoglycoprotein from the unfertilized eggs of rainbow trout (*Salmo gairdneri*), *J. Biol. Chem.* 261 (12) (1986) 5262–5269.
- [30] A. Kameyama, W.W. Thet Tin, M. Toyoda, M. Sakaguchi, A practical method of liberating O-linked glycans from glycoproteins using hydroxylamine and an organic superbase, *Biochem. Biophys. Res. Commun.* 513 (1) (2019) 186–192.
- [31] Y. Yang, R. Murai, Y. Takahashi, et al., Comparative studies of polysialic acids derived from five different vertebrate brains, *Int. J. Mol. Sci.* 21 (22) (2020).
- [32] S.L. Luxembourg, L.A. McDonnell, M.C. Duursma, X. Guo, R.M. Heeren, Effect of local matrix crystal variations in matrix-assisted ionization techniques for mass spectrometry, *Anal. Chem.* 75 (10) (2003) 2333–2341.
- [33] L.J. Rubinstein, K.E. Stein, Murine immune response to the *Neisseria meningitidis* group C capsular polysaccharide. II. Specificity, *J. Immunol.* 141 (12) (1988) 4357–4362.